JCTC Journal of Chemical Theory and Computation

# The Shell Structure of Atoms

Georg Eickerling and Markus Reiher*

*Laboratorium für Physikalische Chemie, ETH Zurich, Hönggerberg Campus, Wolfgang-Pauli-Strasse 10, CH-8093 Zurich, Switzerland*

Received September 24, 2007

**Abstract:** The total electron density distribution of an isolated atom or an atom in a molecule does not reveal an atomic shell structure. Many localization functions, such as the radial averaged electron density, the Laplacian of the electron density, or the electron localization function have been proposed to visualize and analyze the shell structure of atoms. It was found that for light main group elements the correct number of shells is revealed by such functions. Later it was recognized that for heavy main group elements and for transition metals many of these diagnostic tools fail to reveal the full set of electronic shells as expected from the periodic table. In this work we focus on the radial structure of isolated atoms as revealed by the Laplacian of the electron density. We will demonstrate that it is the nodal structure of the orbitals of the inner shells which is responsible for the diminishing of at least one valence shell of third row transition metal atoms. Particular attention is paid to the effect of different electronic configurations on the shell structure of atoms and the question if the changes observed in the Laplacian of the radial density are sufficiently large for experimental studies on the topology of the electron density. Our presentation is as general as possible and, hence, employs a fully relativistic, i.e., four-component picture and a multiconfigurational ansatz for the wave function, which is thus valid for the whole periodic table of elements.

## 1. Introduction

The Aufbau principle for atoms, according to which the electrons in atoms are successively added to form shells and subshells denoted by the principle quantum number $n$ and by the angular quantum number $l$, is one of the central principles in chemistry. Yet, the shell structure of an atom is not directly observable in the total electron density, which is a monotonically decaying function. In ref 19 this is shown to be true for the electron density outside a sphere with a certain radius $r$ and for $r \rightarrow \infty$. For the region close to the core the Kato cusp condition states that the density is monotonic in this region, and although there is still no formal proof,[8] there exists further computational evidence that the atomic density is indeed a monotonically decaying function for all values of $r$.[1−7,9] Therefore, many functions derived from the total electron density have been proposed as a tool to recover the shell structure and to visualize the Aufbau principle. The first studies focused on the radial density distribution function $D(r)$ which was shown to exhibit maxima that correspond to the electronic shells of atoms. In a pioneering study, Bartell and Brockway showed by electron diffraction experiments that for argon atoms three local maxima in $D(r)$ corresponding to the three occupied shells with $n = 1$, 2, and 3 can be found.[20] Theoretical investigations later uncovered that the correct number of maxima can only be observed for elements with nuclear charge smaller than or equal to 18.[21−23]

Therefore, other means have been studied for this purpose like the electron localization function (ELF),[24] the electron localization indicator (ELI),[25] the Laplacian of the electron density,[26,27] or the average local electrostatic potential $V(\boldsymbol{r})/\rho(\boldsymbol{r})$.[28] Of these functions the Laplacian of the electron density has the advantages of (i) not being dependent on any reference definition and (ii) being accessible not only by quantum chemical calculations but also directly from electron density distributions obtained from experiment[29−33] without the use of further approximations or assumptions. We note

* Corresponding author e-mail: markus.reiher@phys.chem.ethz.ch.

10.1021/ct7002447 CCC: $40.75 
Published on Web 01/12/2008

that the first of these points also holds for the one-electron potential[10−12] and the logarithm or the logarithmic derivative of the electron density.[13,14,37] These functions might be used as alternatives for the Laplacian of the electron density in future studies.

The capability of the Laplacian of the total electron density to reveal the shell structure of atoms was first reported by Bader et al. for the second row elements Li to Ne and for the argon atom.[26,27] In two following studies, Sagar et al.[34] and Shi and Boyd[35] investigated the shell structure as revealed by the Laplacian in more detail. The study of Sagar et al. included the elements He to Ba and Lu to Ra, the one by Shi and Boyd the elements Li to Xe.[34,35] In both papers the numerical nonrelativistic wave functions by Clementi and Roetti[36] were employed. The result of these studies was that at most five shells can be observed in the Laplacian in terms of a pair of regions where the Laplacian is positive and negative. Later, Kohout et al. investigated the Laplacian of the electron density obtained from numerical four-component relativistic calculations for the elements of the 2nd, 11th, 12th, 13th, and 14th groups of the periodic table.[37]

These previous studies included only one electronic configuration for each atom. The concept of distinguishing between electronic shells in an atom is, however, conceptually related to the definition of the valence configuration of an atom in a molecule. Both are based on a molecular (or atomic) orbital picture derived from quantum-mechanical many electron theory. It is common practice to base general chemical concepts such as the orbital electronegativity introduced by Hinze and Jaffe on such theoretical grounds.[38−40] But also experimental findings are often interpreted employing these generalized ideas. For instance, Mössbauer spectroscopy can be used to determine the valence configuration of an atom in a molecule.[41] In this case, the conclusions are drawn rather indirectly as the experiment itself is sensitive to the electron density at the position of the nucleus. However, since the total electron density is experimentally accessible for instance by X-ray diffraction experiments, the topological analysis of the Laplacian of the electron density could be a valuable tool to investigate the electronic configuration of an atom in a molecule. The results of experimental studies on the topology of the electron density are in very good agreement with results obtained by quantum chemical calculations,[42−47] and it might be possible to assess the expected changes in the total electron density due to different valence configuration of atoms.

In this work we therefore investigate to which extent the Laplacian of the electron density is sensitive to different electronic configurations of isolated atoms. This requires a thorough understanding of the features revealed by the Laplacian in the valence region of an atom. Therefore, we introduce the spherically averaged electronic density for closed- and open-shell systems calculated in a relativistic framework based on Dirac's four-component one-electron Hamiltonian[48] in section 2. The material presented in this section and in section 3 is designed as a self-contained introduction of the theoretical background necessary for the understanding of the later discussion and might be skipped by the expert reader. We then analyze the shell structure of closed-shell atoms as revealed by the Laplacian in section 4.1. In section 4.2 we will then focus on open-shell atoms by analyzing multiconfiguration wave functions obtained by numerical multiconfiguration self-consistent field (MCSCF) calculations.

## 2. Theoretical Background

The explicit expression from which the electron density is calculated depends on the type of approximation for the wave function from which it is calculated. In the following it is thus necessary to present these expressions for the general case of an MCSCF wave function in a Dirac-based relativistic theory. In addition, the brief presentation of the theoretical foundations in this section shall also unambiguously introduce the notation required.

**2.1. The Spherically Averaged Electron Density.** To derive the spherically averaged electron density, which is a central quantity as it can also be obtained for an atom in a molecule, we will start from the general definition of the electron density $\rho(\boldsymbol{x})$ to be calculated from the total electronic ground state wave function $\Psi_0$ according to

$$\rho(\boldsymbol{x}) = N \int \mathrm{d}\sigma_1 \int_{-\infty}^{\infty} \mathrm{d}^3x_2 \int \mathrm{d}\sigma_2 \ldots \int_{-\infty}^{\infty} \mathrm{d}^3x_N \int \mathrm{d}\sigma_N \; \Psi_0^{\dagger}(\boldsymbol{x}, \sigma_1, \boldsymbol{x}_2, \sigma_2, \ldots, \boldsymbol{x}_N, \sigma_N)\Psi_0(\boldsymbol{x}, \sigma_1, \boldsymbol{x}_2, \sigma_2, \ldots, \boldsymbol{x}_N, \sigma_N) \quad (1)$$

where $\boldsymbol{x}_i$ denotes the spatial coordinates and $\sigma_i$ the spin coordinates. $\rho(\boldsymbol{x})$ is only a function of three Cartesian coordinates $\boldsymbol{x} = (x_1, x_2, x_3)$. However, for the derivation of a spherically averaged electron density for an atom in a molecule one most conveniently uses a representation in the polar coordinates $\boldsymbol{r} = (r, \varphi, \vartheta)$. Thus, in a first step we seek to find a *radial* electron density $D(r)$ that only depends on the radial coordinate $r$ and for which holds

$$\int_0^{\infty} \mathrm{d}r D(r) \equiv N \quad (2)$$

Comparing this definition with the integration of $\rho(\boldsymbol{r}) = \rho[\boldsymbol{r}(\boldsymbol{x})]$ and noting that $\mathrm{d}^3x = \mathrm{d}x_1\, \mathrm{d}x_2\, \mathrm{d}x_3 = r^2\, \mathrm{d}r \sin\vartheta\, \mathrm{d}\vartheta\, \mathrm{d}\varphi$

$$\int_{-\infty}^{\infty} \mathrm{d}^3x \rho(\boldsymbol{x}) = \int_0^{\infty} r^2 \mathrm{d}r \int_0^{2\pi} \int_0^{\pi} \sin\vartheta\, \mathrm{d}\vartheta\, \mathrm{d}\varphi\, \rho[\boldsymbol{r}(\boldsymbol{x})] = N \quad (3)$$

we find

$$D(r) = r^2 \int_0^{2\pi} \int_0^{\pi} \sin\vartheta\, \mathrm{d}\vartheta\, \mathrm{d}\varphi\, \rho[\boldsymbol{r}(\boldsymbol{x})] \quad (4)$$

In order to define a density which may serve our purposes for an atom in a general molecule as well as for a spherically symmetric atom, we need to define a spherically averaged density $\bar{\rho}(r)$ that is the total (electronic) charge in a spherical shell with inner radius $r$ and thickness $\mathrm{d}r$, i.e., $D(r)\mathrm{d}r$, divided by the volume of this shell $(4\pi r^2\mathrm{d}r)$

$$\bar{\rho}(r) = \frac{D(r)\mathrm{d}r}{4\pi r^2 \mathrm{d}r} = \frac{D(r)}{4\pi r^2} \quad (5)$$

so that integration over all shells, $\int \bar{\rho}(r) 4\pi r^2 \mathrm{d}r = N$, still yields the total number of electrons. This spherically averaged electron density $\bar{\rho}(r)$ is the quantity one should consider for the investigation of atomic properties when discussing

the electron density along a radial ray in an atom or in an atom of a molecule.

**2.2. Wave Function of Spherically Symmetric Atoms.** In the following we will give a brief introduction into the notation needed for our discussion of the spherically averaged electron density $\bar{\rho}(r)$ for atoms with closed- and open-shell configurations. We start from the general representation of the ground state wave function $\Psi_0$ as a linear combination of configuration state functions $\Phi_I$

$$\Psi_0 = \sum_{I=1}^{m} \Phi_I C_I \tag{6}$$

For $m = \infty$ the result is the exact full configuration interaction (CI) solution. Each configuration state function $\Phi_I$ is constructed from antisymmetrized products of one-electron functions, the orbitals $\psi_i(\boldsymbol{x})$. For finite $m$ one aims for an MCSCF solution, since orbital relaxation needs to be taken into account. This requires an optimization of the one-particle basis within the truncated CI expansion. For $m = 1$ one would obtain the Hartree−Fock solution. In this case the many-electron function $\Phi_1$ reduces to a single Slater determinant. In the case of atoms the orbitals are either the one-component atomic orbitals[49]

$$\psi_i(\boldsymbol{x}, \sigma) \rightarrow \psi_{n_i l_i m_{l,i}}(\boldsymbol{r}, \sigma) = \frac{P_{n_i l_i(r)}}{r} Y_{l_i m_{l,i}}(\vartheta, \varphi)\chi(\sigma) \tag{7}$$

of nonrelativistic Schrödinger quantum mechanics or the four-component spinors[50]

$$\psi_i(\boldsymbol{x}) \rightarrow \psi_{n_i \kappa_i m_{j,i}}(\boldsymbol{r}) = \frac{1}{r}\begin{pmatrix} P_{n_i \kappa_i(r)}\chi_{\kappa_i m_{j,i}}(\vartheta, \varphi) \\ iQ_{n_i \kappa_i(r)}\chi_{\kappa_i m_{j,i}}(\vartheta, \varphi) \end{pmatrix} \tag{8}$$

of the Dirac theory of the electron ($\kappa_i$ is the four-component analog to the angular momentum quantum number $l$ and $m_{j(i)}$ is the eigenvalue of the $z$ -component $\hat{j}_z$ of the one-electron total angular momentum operator). In the former case, the atomic configuration state functions $\Phi_I$ are eigenfunctions of the total spin operators $\hat{\boldsymbol{L}}^2$, $\hat{L}_z$, $\hat{\boldsymbol{S}}^2$, and $\hat{\boldsymbol{S}}_z$, while in the latter case they are eigenfunctions of $\hat{\mathbf{J}}$ and $\hat{J}_z$. In general, one obtains the electron density from eq 1 using eq 6 as

$$\rho(\boldsymbol{x}) = \sum_{ij}^{k} \gamma_{ij}\psi_i^\dagger(\boldsymbol{x})\psi_j(\boldsymbol{x}) \tag{9}$$

for any of the above introduced representations of the one-electron functions. Here, $k$ is the total number of orbitals, and $\{\gamma_{ij}\}$ is the first-order density matrix. The density matrix elements are given by

$$\gamma_{ij} = \langle \Psi_0 | \hat{E}_{ij} | \Psi_0 \rangle = \langle a_i \Psi_0 | a_j \Psi_0 \rangle \tag{10}$$

where the excitation operator in second quantization reads[51]

$$\hat{E}_{ij} = a_i^\dagger a_j \tag{11}$$

and operates on spin orbitals or spinors, respectively. Note that we have taken advantage in eq 10 of the fact that the adjoint operator of the creator $a_i^\dagger$ is the annihilator $a_i$. Invoking the formalism of second quantization thus allows us to conveniently bury the integration of eq 1 over $N - 1$ coordinates in the matrix element $\langle \Psi_0 | \hat{E}_{ij} | \Psi_0 \rangle$. It should be noted that the resulting configuration state functions ($a_i \Phi_I$) are many-particle basis functions for ($N - 1$) electrons and fulfill all properties that are also fulfilled by the parental $\Phi_I$ basis functions.

Expressing $\Psi_0$ in eq 10 by the linear combination of configuration state functions $\Phi_I$ from eq 6 then yields

$$\gamma_{ij} = \sum_{IJ} C_I C_J \langle \Phi_I | \hat{E}_{ij} | \Phi_J \rangle = \sum_{IJ} C_I C_J \langle a_i \Phi_I | a_j \Phi_J \rangle \tag{12}$$

where we assumed the CI expansion coefficients $C_I$ to be real. In the Hartree−Fock case with $m = 1$ eq 9 simplifies to a single summation with $C_I = C_J = 1$, and the diagonal density matrix elements become the occupation numbers

$$\gamma_{ij} \rightarrow \gamma_{ii} = \langle \Phi_1 | \hat{E}_{ii} | \Phi_1 \rangle = \begin{cases} 0 \text{ or } 2 & \text{nonrelativistic} \\ 0 \text{ or } 1 & \text{four-component} \end{cases} \tag{13}$$

due to the orthogonality of the one-electron functions $\psi_i$ from which $\Phi_1$ is constructed. This illustrates explicitly that the integral described by the brackets in eq 12 using the annihilation operators to annihilate one orbital from $\Phi_1$ is equivalent to the integration over all but one electronic coordinate in eq 1. In addition, we should emphasize that in the nonrelativistic theory the last equation refers to the special case of a closed-shell electronic structure such that the excitation operator reads

$$E_{ij} = a_{i\alpha}^\dagger a_{j\alpha} + a_{i\beta}^\dagger a_{j\beta} \tag{14}$$

We now proceed by transforming $\rho(\boldsymbol{x})$ as given in eq 9 from Cartesian to polar coordinates. In the case of atoms, the angular degrees of freedom can be integrated out analytically, so that we get an explicit expression for $D(r)$ of eq 4

$$D(r) = \sum_{ij} \gamma_{ij} D_{ij}(r) \times \begin{Bmatrix} \langle Y_{l_i m_i} | Y_{l_j m_j} \rangle \\ \langle \chi_{\kappa_i m_{j,i}} | \chi_{\kappa_j m_{j,j}} \rangle \end{Bmatrix} = \sum_i \gamma_{ii} D_{ii}(r) \tag{15}$$

where

$$D_{ij}(r) = \begin{cases} P_i(r)P_j(r) & \text{nonrelativistic} \\ P_i(r)P_j(r) + Q_i(r)Q_j(r) & \text{four-component} \end{cases} \tag{16}$$

According to eq 5, the spherically averaged density then reads

$$\bar{\rho}(r) = (4\pi r^2)^{-1} D(r) = \begin{cases} (4\pi r^2)^{-1} \sum_{ij} \gamma_{ij} P_i(r) P_j(r) & \text{nonrelativistic} \\ (4\pi r^2)^{-1} \sum_{ij} \gamma_{ij} [P_i(r)P_j(r) + Q_i(r)Q_j(r)] & \text{four-component} \end{cases} \tag{17}$$

and is given in particles per bohr$^3$.

**2.3. Closed-Shell Configurations.** In the special case of closed-shell molecules with $N$ electrons represented by a single Slater determinant the general expression for $\rho(\boldsymbol{x})$ given in eq 9 simplifies in the nonrelativistic theory to

$$\rho(\boldsymbol{x}) = \sum_{i}^{N/2} 2\psi_i^{\dagger}(\boldsymbol{x})\psi_i(\boldsymbol{x}) \tag{18}$$

and in case of the four-component relativistic theory to

$$\rho(\boldsymbol{x}) = \sum_{i}^{N} \psi_i^{\dagger}(\boldsymbol{x})\psi_i(\boldsymbol{x}) \tag{19}$$

if no additional symmetries (like spherical or point group symmetry) are exploited. In the case of atoms with *nsh* subshells, the equivalence restriction of one and the same radial function eqs 7 and 8 per subshell ($nl$) or ($n\kappa$), respectively, allows us to simplify eq 17 even further, and we obtain for the radial and the spherically averaged densities

$$\bar{\rho}(r) = \sum_{i}^{nsh} d_i \frac{D_{ii}(r)}{4\pi r^2} \tag{20}$$

with the subshell occupation numbers

$$d_i = \begin{cases} 2l_i + 1 & \text{nonrelativistic} \\ 2|\kappa_i| & \text{four-component} \end{cases} \tag{21}$$

**2.4. Minimal Model for Open-Shell Structures and Near-Degenerate Configurations.** The CI expansion of eq 6 allows us to identify important electronic configurations, i.e., those with large CI coefficients $C_I$. In the case of two equally important open-shell configurations ($m = 2$) the general expression for $\rho(\boldsymbol{x})$ given in eq 9 reduces to

$$\rho(\boldsymbol{x}) = \sum_{ij}^{N+1} \gamma_{ij}\psi_i^{\dagger}(\boldsymbol{x})\psi_i(\boldsymbol{x}) \tag{22}$$

if these two configurations differ by only one orbital. The summation runs over all spin orbitals or spinors, respectively, that enter the two CSFs.

**2.5. The Laplacian of the Radial Density.** The shell structure of isolated atoms has been previously investigated by means of $D(r)$ and by analyzing the Laplacian $\nabla^2$ of the electron density. The Laplacian operator in spherical coordinates is given by[52]

$$\nabla^2 = \frac{1}{r^2}\frac{\partial}{\partial r}\left(r^2\frac{\partial}{\partial r}\right) + \frac{1}{r^2\sin\vartheta}\frac{\partial}{\partial\vartheta}\left(\sin\vartheta\frac{\partial}{\partial\vartheta}\right) + \frac{1}{r^2\sin^2\vartheta}\frac{\partial^2}{\partial\varphi^2} \tag{23}$$

The spherically averaged density $\bar{\rho}(r)$ does not depend on the angular coordinates so that all partial derivatives with respect to $\vartheta$ and $\varphi$ vanish, and thus the Laplacian for this special case simplifies to

$$\nabla^2\bar{\rho}(r) = \frac{1}{r^2}\frac{d}{dr}\left(r^2\frac{d}{dr}\right)\bar{\rho}(r) = \frac{d^2}{dr^2}\bar{\rho}(r) + \frac{2}{r}\frac{d}{dr}\bar{\rho}(r) \tag{24}$$

## 3. Computational Methodology

Atomic four-component Dirac−Hartree−Fock and MCSCF calculations were carried out fully numerically.[53] While all angular degrees of freedom are treated analytically, the two radial functions $P_i(r) = P_{n_i\kappa_i}(r)$ and $Q_i(r) = Q_{n_i\kappa_i}(r)$ of the 4-spinor are represented on an equidistant, logarithmic grid of points in the new variable $s$, which is calculated from the original radial variable $r$ (see refs 54 and 55 for details on this type of radial grid). The Laplacian of the spherically averaged electron density was calculated numerically employing a three-point finite difference formula. Concerning the definition of a shell we will use the notation convention to define a shell by the principal quantum number $n$ rather than by a pair of quantum numbers ($n$,$l$), which we denote a subshell.

**3.1. Peculiarities of Numerical Solution Methods.** For atomic structure calculations the use of an equidistant grid in $r$ for the representation of the radial functions $P_i$ and $Q_i$ is not efficient. Therefore one uses a variable transformation to a new variable $s(r)$ which generates an equidistant grid in $s$ which corresponds to a grid in $r$ with small step sizes $h$ for small values of $r$ and larger step sizes for larger values of $r$.[54] The function $s(r)$ for a logarithmic grid used in this work is[55]

$$s(r) = \frac{1}{T}[\ln(r + b) - \ln b] \tag{25}$$

In this equation, $T^{-1}$ is a normalization factor which ensures that $s(r_{\max}) = 1$. The value $r_{\max}$ defines a sphere in which the atom is confined, and the parameter $b$ is used to vary the distribution of grid points on the logarithmic grid.

To calculate the Laplacian in this new radial variable $s(r)$ one needs to transform eq 24 to the new coordinate $s$. This means we need to rewrite the derivative[55]

$$\frac{d}{dr} = \left(\frac{ds}{dr}\right)\frac{d}{ds} \equiv w^2\frac{d}{ds} \tag{26}$$

where we introduced $w^2$ as the square of the weighting function $w(s)$.

For the first term of the sum on the right-hand side of eq 24, we obtain the operator identity[55]

$$\frac{d^2}{dr^2} = w^2\frac{d}{ds}\left(w^2\frac{d}{ds}\right) = w^3\left[\frac{d^2}{ds^2}w - \left(\frac{d^2w}{ds^2}\right)\right] \tag{27}$$

The Laplacian of the *spherically averaged* radial density [bohr$^{-3}$] in the new radial variable $s$ is then given by

$$\nabla^2\bar{\rho}(r) = \left\{w^3\left[\frac{d^2}{ds^2}w - \left(\frac{d^2w}{ds^2}\right)\right] + \frac{2}{r}w^2\frac{d}{ds}\right\}\bar{\rho}(r)[\text{bohr}^{-5}] \tag{28}$$

The multiplication with the elementary charge $e$ which would convert the electron density into the (positive) charge density distribution of $N$ elementary charges has not been made explicit. The negative charge density would then be obtained by multiplication with (−1). The Laplacian of the (negative) charge density, which corresponds to the negative Laplacian of the electron density, is then defined as

$$L(r) = -e\nabla^2\bar{\rho}(r) = -\sum_{ij}\frac{1}{4\pi r^2}\nabla^2 D_{ij}[\text{e bohr}^{-5}] \tag{29}$$

so that local concentration of charge corresponds to positive values of $L(r)$. For unit conversion to eÅ$^{-5}$ the results

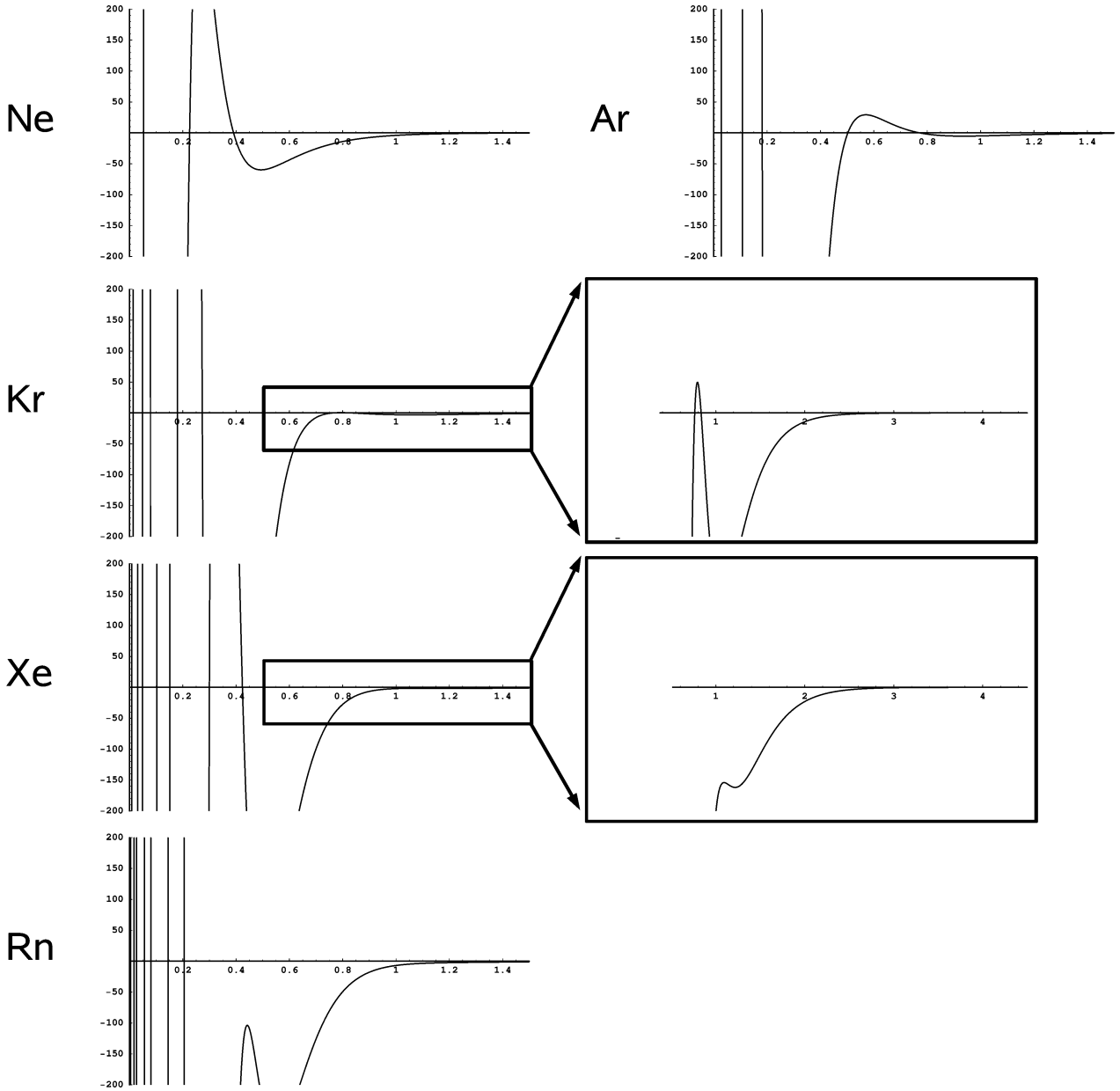


***Figure 1.*** Negative Laplacian of the spherical averaged radial density $L(r)$ of the rare gases Ne−Rn. Comparing the heights of the outermost maxima in $L(r)$ demonstrates the systematic diminishing of the valence shell charge concentration. In the case of Xe the valence shell is only resolved as a local maximum in the negative region of $L(r)$. Units are in eÅ$^{-5}$ on the ordinate and Å on the abscissa. Note the different minimal and maximal values used for the plots for Ne−Rn (−200 to 200 eÅ$^{-5}$ and 0 to 1.5 Å) and the two expanded views for Kr and Xe (−2 to 2 eÅ$^{-5}$ and 0 to 4.5 Å).

obtained in Hartree atomic units were multiplied by a conversion factor of 24.098731 Å$^{-5}$. Concerning $\rho(r)$ we note that values given in eÅ$^{-3}$ denote a fraction of electrons per cubic angstrøm.

## 4. Results and Discussion

**4.1. Vanishing Valence Shell Structure with Increasing Nuclear Charge.** We first consider the shell structure of the closed-shell rare-gas atoms Ne to Rn (the simple case of the He atom with only a single shell has been left aside). Figure 1 depicts $L(r)$ of the electron density in a range of $r$ from 0 to 1.5 Å. From Ne to Kr $L(r)$ resolves the complete electronic shell structure with 2, 3, and 4 pairs of positive and negative regions of $L(r)$ for Ne, Ar, and Kr, respectively. However, it is obvious from the height of the maxima found for the outermost shell that the degree of local charge concentration, indicated by a positive value of $L(r)$, is systematically reduced with increasing atomic number $Z$ ($L(r) = 369$, 29, 0.5, and $-1.5$ eÅ$^{-5}$ for Ne, Ar, Kr, and Xe, respectively).

The reason for the diminishing of the valence shell can be studied considering the Ne atom. Figure 2 depicts the contributions to $L(r)$ due to the $n = 1$ (a) and the $n = 2$ shell (b) together with the total $L(r)$ (c). The maximum of the valence shell at approximately $r = 0.2$ Å ($L(r) = 1325$ e Å$^{-5}$) is significantly shifted ($r = 0.26$ Å) and reduced in height ($L(r) = 369$ eÅ$^{-5}$) by the negative contribution of the 1*s* shell in this region. Recall that the Laplacian is a linear operator that allows us to simply add up the individual shell

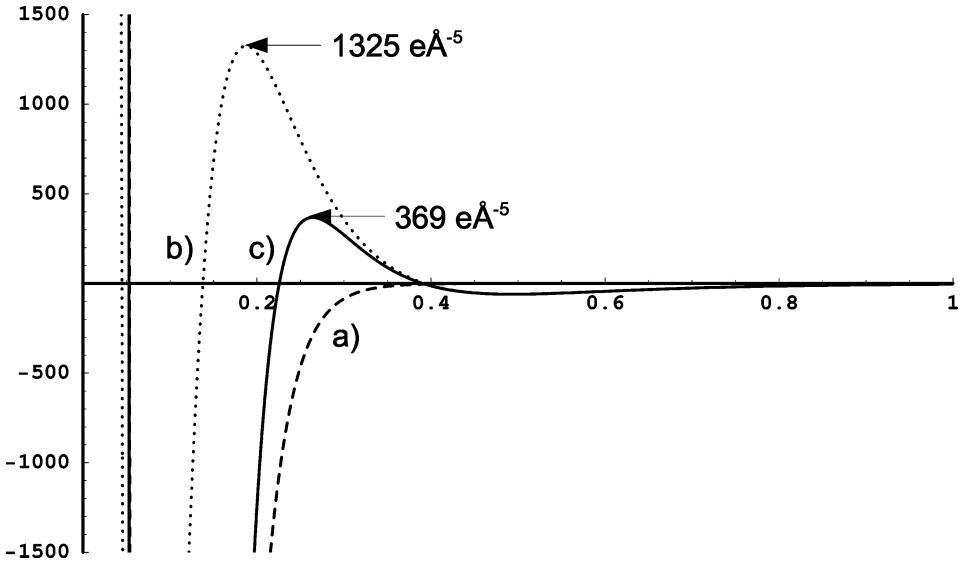


***Figure 2.*** Contributions to the negative Laplacian of the spherical averaged radial density $L(r)$ of (a) the ($n = 1$) shell (dashed line), (b) the ($n = 2$) shell (dotted line), and (c) the total $L(r) = -(4\pi r^2)^{-1} \sum_{i\in\{1s,2s,2p\}} \nabla^2 D_{ii}$ of a Ne atom (solid line). Units are in eÅ$^{-5}$ on the ordinate and Å on the abscissa.

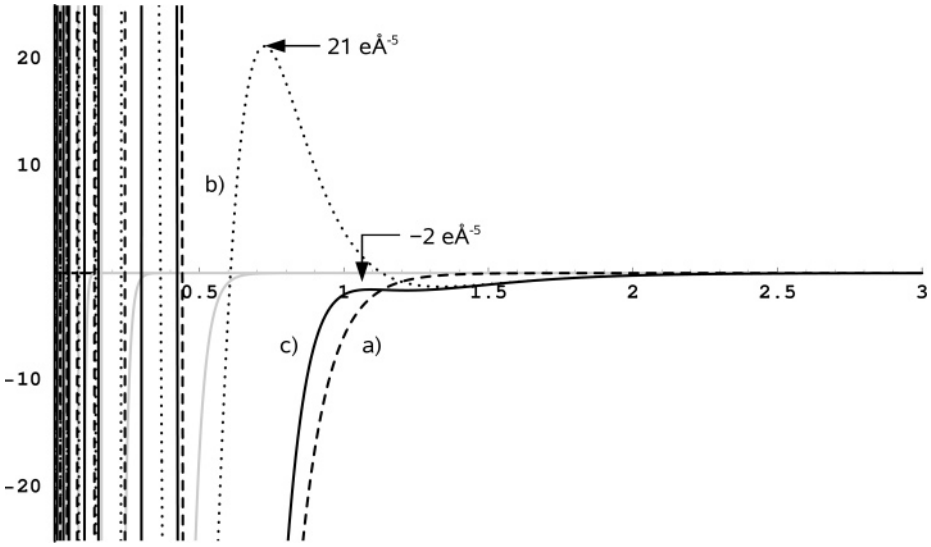


***Figure 3.*** Decomposition of the total Laplacian $L(r)$ of a Xe atom in terms of individual shell contributions (compare eq 29); (a) ($n = 4$) shell (dashed line), (b) ($n = 5$) shell (dotted line), and (c) total $L(r)$ (solid line). The sums of the contributions of the ($n = 1$, 2, and 3) shells are indicated by light gray lines. Units are in eÅ$^{-5}$ on the *y*- and Å on the *x*-axis.

and subshell contributions. Thus, the maximum found for a shell $n$ is not a feature solely to be ascribed to one electronic shell. In fact, the height of the maximum in $L(r)$ and also its position in $r$ is to a large extent affected by the penultimate ($n - 1$) shell.

Accordingly, the reason why only a weak shoulder in the *negative* region of $L(r)$ can be observed for the $n = 5$ valence shell of Xe lies in the contributions from the $n = 4$ shell. Figure 3 depicts the same scenario for Xe as has been discussed before for Ne. The still pronounced, yet compared to the ($n = 2$) valence shell in Ne weaker maximum in $L(r)$ due to the $n = 5$ valence shell orbitals (dotted line in Figure 3) is severely reduced by the region of charge depletion of the ($n - 1$) shell (dashed line in Figure 3). Figure 3 also depicts the contributions of the $n = 1$, 2, and 3 shell (light gray lines). As can be seen, $L(r)$ for these three shells already reached values very close to zero in the region around $r =$ 1 Å so that the ($n - 2$) and lower lying shells do not significantly affect the valence shell maximum. At the same time, the maximum in the negative region of the total $L(r)$ is shifted further away from the nucleus, relative to the maximum of the valence shell contribution only. Comparing Figures 2 and 3 it is obvious that it is indeed only the right-hand side tail and thus only a small part of the maximum in $L(r)$ of the valence shell which is remaining as a signature of a valence shell maximum. Thus, not only the magnitude but also the positions of the minima and maxima attributed to one electronic shell are affected by the underlying shells.

The reduction of local charge concentration with increasing nuclear charge number $Z$ due to the contribution from the ($n - 2$) shell is also visible for the ($n - 1$) shell. The corresponding local maximum in $L(r)$ is becoming weaker as $Z$ increases from He to Xe: It reduces from 19 377 eÅ$^{-5}$ in Ar to 8199 eÅ$^{-5}$ in Kr and to 1807 eÅ$^{-5}$ in Xe. Moving

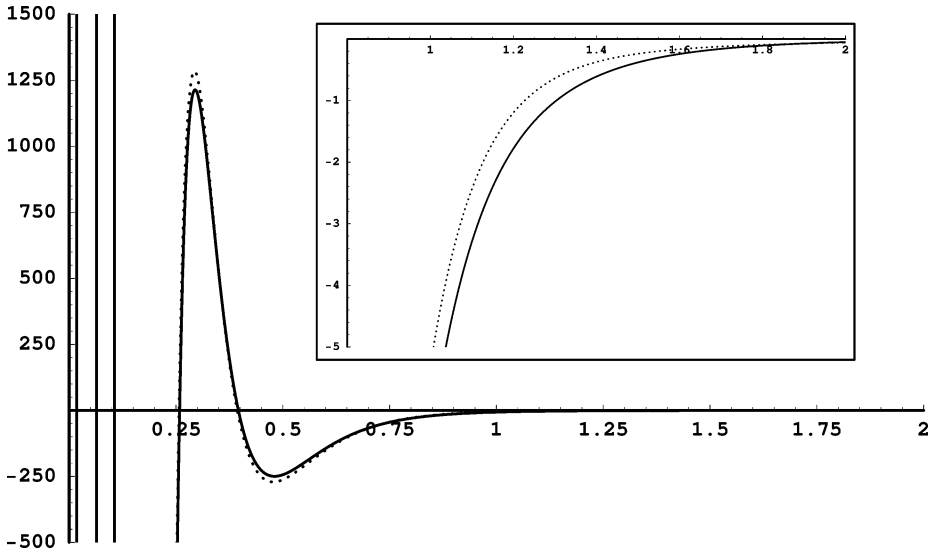


***Figure 4.*** Negative Laplacian of the spherically averaged radial density of a Ni atom with $4s^0\ 3d^{10}$ configuration (solid line) and $4s^2\ 3d^8$ configuration (dotted line). Units are in eÅ$^{-5}$ on the *y*- and Å on the *x*-axis. The inlay shows an enlarged view of the region −5 to 0 eÅ$^{-5}$ and 0 to 2 Å.

finally from Xe to Rn, there is a severe drop in the value of $L(r)$ to −104 eÅ$^{-5}$. This large decrease is caused by the additional *f*-subshell which is now occupied for the first time. When subtracting the contribution from the 4*f* orbitals to the total $L(r)$, the maximum for the $(n = 5)$ shell for Rn increases to 585 eÅ$^{-5}$, but still no maximum or shoulder which could be attributed to the $(n = 6)$ shell can be detected.

The results presented so far illustrate that when counting and interpreting stationary points in the Laplacian of the radial density as electronic shells one must keep in mind that always the $(n - 1)$ shell significantly affects the *n*th shell, leading for $n > 3$ to the possibility of maxima in the negative region of $L(r)$ or even a complete absence of a local maximum. Now the question arises which feature is indicative of a shell in the Laplacian. Based on similar results, Sager et al. suggested in their study not to use the minima or maxima, but the zero crossings following a maximum as indicators for the atomic shell structure as their positions correlate well with the radius $(n^2/Z)[\hbar/(m_e e^2)]$ from Bohr's theory.[34] But this interpretation would then rule out to count the maximum in the *negative* region of $L(r)$ as indicative for the $n = 5$ shell in Xe.

Other authors used the occurrence of a local maximum followed by a local minimum in $L(r)$ as an indicator for a shell.[37] This criterion is based on the interpretation of a positive sign of $L(r)$ as a local charge concentration which can be rationalized by the ratio of the kinetic and the potential energy density given by the virial theorem for an atom in a molecule as derived by Bader[56]

$$\nabla^2\rho(\boldsymbol{r}) = 2G(\boldsymbol{r}) + V(\boldsymbol{r}) \tag{30}$$

According to this, the charge is locally concentrated at a given position $\boldsymbol{r}$ if the potential energy density $V(\boldsymbol{r})$, which is a negative-valued function, dominates the positive kinetic energy density $G(\boldsymbol{r})$ by at least a factor of 2, meaning that the energy of the electrons is dominated by the potential energy at $\boldsymbol{r}$. If on the contrary $\nabla^2\rho(\boldsymbol{r})$ is positive (and thus $L(\boldsymbol{r})$ negative), then the kinetic energy dominates, and a region of charge depletion is assumed. With respect to this interpretation of the sign of $L(\boldsymbol{r})$ the diminishing of the valence shell maximum corresponds to a reduction of the local charge concentration until the ratio of $G(\boldsymbol{r})$ and $V(\boldsymbol{r})$ is smaller than two as observed in the case of Xe. However, this could still mean that the absolute value of $V(\boldsymbol{r})$ is larger than that of $G(\boldsymbol{r})$. One must be aware of the fact that eq 30 and the interpretation given above is only valid for a specific choice of the local kinetic energy density. For a detailed discussion see, for example refs 15−18.

As we will demonstrate in the following sections, the maxima found in the negative region of $L(r)$ indeed contain information on the electronic configuration of an atom. The counting of zero crossings alone would rule out an interpretation of these features as indicative for the shell structure. Therefore, keeping in mind the fact that a maximum in $L(r)$ for a given shell *n* is always (also for light elements) affected by the penultimate shell $(n - 1)$, in the following discussion we will assume that any kind of local maximum (and, hence, also in the negative regions of $L(r)$) is indicative for a shell of a atom.

**4.2. Open-Shell Atoms.** After discussing the general features of the Laplacian in the valence shell of closed-shell rare-gas atoms we will now proceed by considering transition metals with $4s^n3d^{10-n}$ configuration in order to understand under which circumstances the fourth shell generated by the 4*s* orbital shows up in $L(r)$. We start the discussion of open-shell systems by considering $L(r)$ of a typical transition metal, namely the nickel atom. For elements of the first transition row one would expect to find four shells in the Laplacian of the spherically averaged electron density. However, when looking at the $4s^0\ 3d^{10}$ and at the $4s^2\ 3d^8$ configuration in separate open-shell calculations as depicted in Figure 4 one finds only *three* pairs of maxima and minima in *both* cases. Of course, in the case of the $4s^0\ 3d^{10}$ configuration only the three shells $n = 1$, 2, and 3 are occupied. But for the $4s^2\ 3d^8$

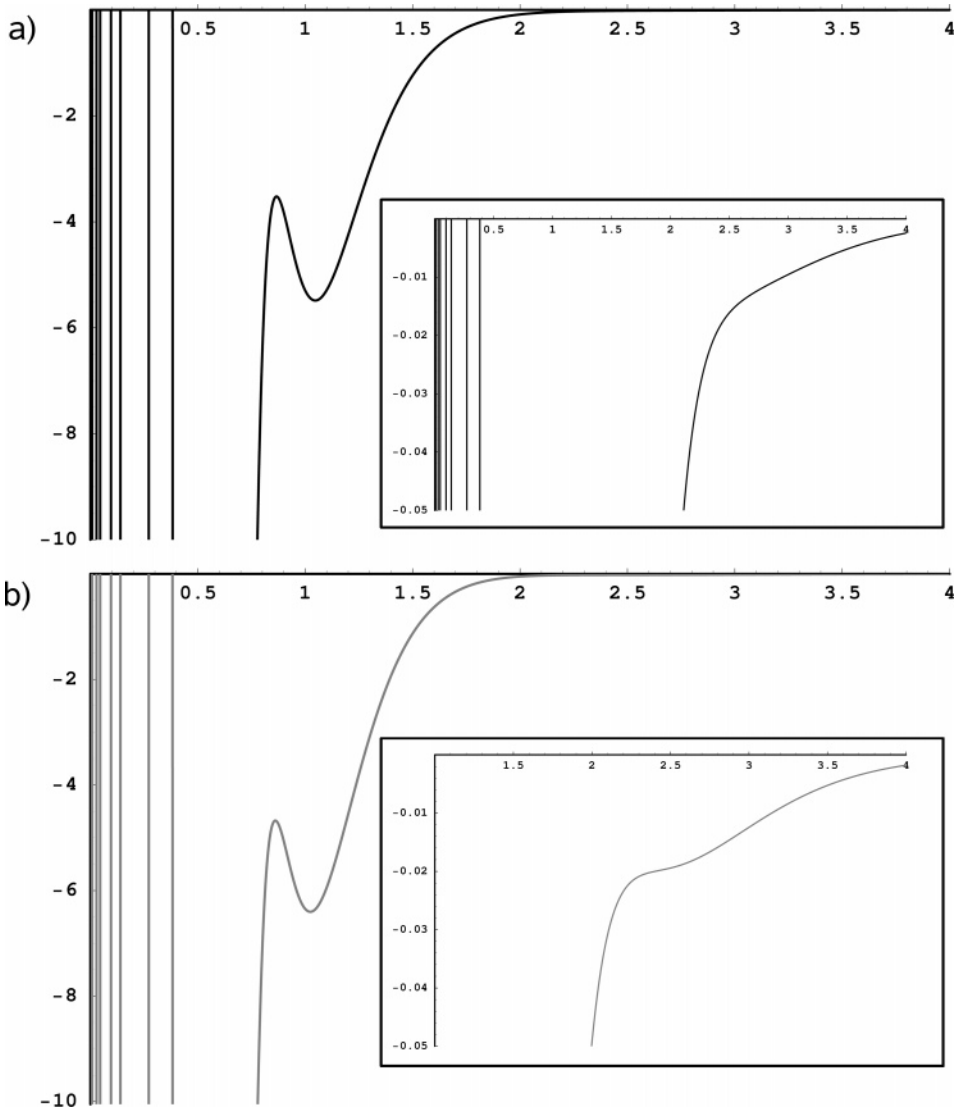


***Figure 5.*** Negative Laplacian $L(r)$ in eÅ$^{-5}$ of the spherically averaged radial density $\bar{\rho}(r)$ of a La atom with $5d^16s^2$ single CSF configuration (a) and of a $La^+$ cation (b). The distance on the $x$-axis is measured in Å. The inlays show an enlarged view of the region $-0.03$ to 0 eÅ$^{-5}$ and 0 to 4 Å.

configuration only three instead of four maxima are found in $L(r)$. The differences due to the different electronic configuration are very small. For instance, the outermost maximum of $L(r)$, denoting the third shell, is more pronounced in the case of the $4s^2\ 3d^8$ than in the case of the $4s^0\ 3d^{10}$ configuration (1284 compared to 1214 eÅ$^{-5}$, respectively). A difference can also be observed in the region at about $r = 1$ Å where one would expect the valence shell maximum in $L(r)$. No additional maximum or shoulder can be found if the 4*s* shell is occupied, only a steeper increase to a less negative value of $L(r)$ is found, which again demonstrates the significant contribution of the $(n-1)$ shell to the valence region of the total Laplacian. An MCSCF calculation which optimizes both of these $J = 0$ configurations simultaneously confirms this picture.

Up to now all calculations were done using a single reference wave function. Especially in the case of open-shell transition metals the description by a single Slater determinant is inadequate. We thus need to look for an example of a transition metal in which two configurations contribute significantly to the total wave function of the atom. The nickel atom is not a good example in this respect as the contribution of the ground state configuration of $4s^0\ 3d^{10}$ clearly dominates in an MCSCF calculation over the contribution of a $4s^2\ 3d^8$ configuration. The first excited-state configuration of a Ni atom starting from a $^3F$ ground state (with $J = 4$) to couple is a $^1G$ state with $4s^2\ 3d^8$ configuration which are energetically separated by approximately 264 kJ mol$^{-1}$.[57] The contribution of this configuration to the total wave function is too small to have an effect on the resulting electron density. In the following section we will therefore investigate a special case for which the energy gap between the electronic ground state and the first excited state is much smaller according to atomic spectroscopy.

**4.3. Two Electronic Configurations Contributing Equally to the Total Density.** In order to identify a case where two electronic configurations become equally important in a CI expansion, we may consider the data from atomic spectroscopy provided by the Moore tables.[57] It turns out that the electronic ground state of the lanthanum atom exhibiting a $5d^16s^2$ configuration with $J = 3/2$ and the first excited-state

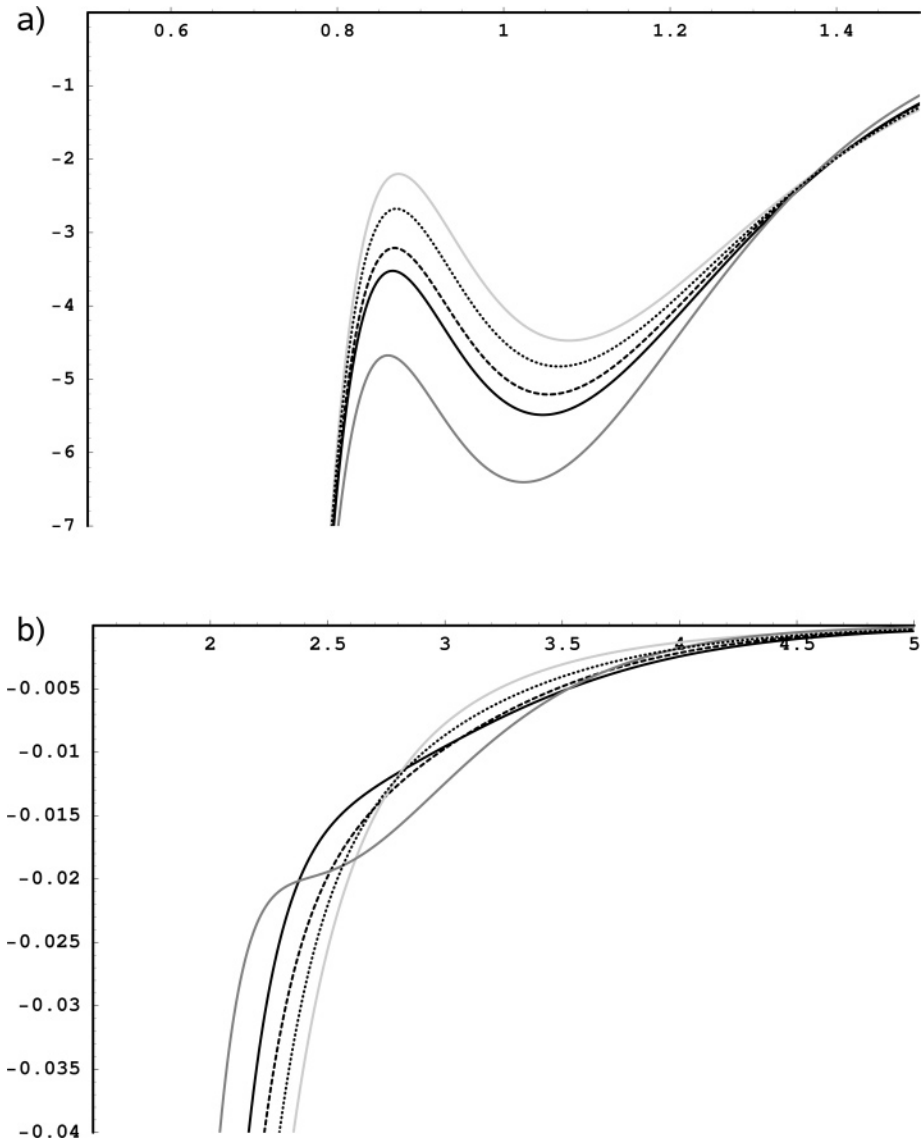


***Figure 6.*** Two selected sections of the negative Laplacian $L(r)$ in eÅ$^{-5}$ of the spherically averaged radial density $\bar{\rho}(r)$ of a La atom at $r \in [0.5,1.5]$ and at $r \in [1.5,5.0]$. Depicted are the results for the $5d^16s^2$ single CSF configuration (black curve), $5d^26s^1$ configuration (dotted curve), $5d^36s^0$ configuration (light gray curve), and the MCSCF superimposed $5d^16s^2$, $5d^26s^1$ configurations (dashed curve). In addition, $L(r)$ of a $La^+$ cation with $5d^06s^2$ is shown (dark gray curve). Distances on the $x$-axis in Å.

with the same $J$ to couple with the ground state are only separated by 32 kJ mol$^{-1}$.[57] Lanthanum is therefore very well suited for the purpose of studying the effect of two equally important configurations on the electron density. We performed several calculations in order to compare the effect of the electronic configuration on the electron density and its Laplacian, starting from a calculation using only one CSF with a $5d^16s^2$ ($J = 3/2$) configuration. In this case $L(r)$ features four maxima with $L(\boldsymbol{r}) > 0$ and one additional fifth maximum in the negative region of $L(\boldsymbol{r})$ (see Figure 5a). This is in accordance with the results discussed in the previous sections. Due to the contribution of the very diffuse 5*d* shell to the total Laplacian the two 6*s* electrons do not give rise to an additional maximum which could be attributed to the sixth shell (see inlay in Figure 5a). That only a single *d*-electron is sufficient for the maximum of the sixth shell to disappear can be demonstrated by considering the negative Laplacian of the cation $La^+$ with a $5d^06s^2$ configuration where an additional shoulder is found at approximately 2.4 Å from the nucleus (see Figure 5b). Obviously, the contribution of the remaining electrons in the fifth shell to the total Laplacian still prevents the formation of a distinct local maximum for the $n = 6$ valence shell. At the same time the maximum in the negative region of $L(r)$ at $r = 0.95$ Å is less pronounced compared to the neutral La atom ($-4.68$ and $-3.52$ eÅ$^{-5}$, respectively). When, in contrast to the cation, which features no 5*d* electrons, assuming a $5d^36s^0$ ($J = 5/2$) configuration, $L(r)$ in the region of this latter maximum is less negative resulting in a maximal value of $-2.20$ eÅ$^{-5}$ (see Figure 6). The negative Laplacian of the neutral La atom with two *s* and one *d* electron in its electronic ground state is found in between these two limiting cases. Finally considering the configuration $5d^26s^1$, we obtain $L(r) = -2.68$ eÅ$^{-5}$ which is an intermediate value between the ones of the $5d^16s^2$ and the $5d^36s^0$ configuration (see Figure 6). Summarizing the results presented so far we note that with an increasing number of *d* electrons in the $n = 5$ shell the maximum in $L(r)$ attributable to the fifth shell becomes less negative.

Considering the difference between the maximum and the minimum the corresponding values follow the same trend, 2.27, 2.15, 1.96, and 1.73 eÅ$^{-5}$ for the $5d^36s^0$, $5d^26s^1$, $5d^16s^2$, and the $5d^06s^2$ configurations, respectively.

This suggests that the Laplacian of the electron density, although not able to fully resolve the shell structure of the La atom as distinct maxima, still provides some information on the electronic configuration of an atom. To investigate this matter further we will in the following compare the results of the single-CSF open-shell calculation to calculations including two CSFs within an MCSCF calculation. Therefore, we performed a calculation employing a $5d^16s^2$ and a $5d^26s^1$ configuration. The resulting CI coefficients are found to be 0.7230 and 0.6909 for the two CSFs, respectively, indicating that both configurations contribute to a similar extent to the final electronic state with $J = 3/2$. The negative Laplacian of the electron density obtained from this calculation also shows the weak maximum at approximately $r = 0.95$ Å ($L(r) = -3.21$eÅ$^{-5}$) which is positioned between the curves obtained for the pure $5d^16s^2$ and the pure $5d^26s^1$ configuration. The same is true considering the value of the difference between the minimum and the maximum (2.00 eÅ$^{-5}$).

Thus, the Laplacian of the electron density is sensitive to the electronic configuration of an atom such that an admixture of approximately 50% of a configuration measured in terms of the (squared) CI coefficients results in a noticeable difference in its course. The relative changes described above follow a clear trend: Starting from a $5d^06s^2$ configuration where the maximum corresponding to the fifth shell is only weakly pronounced, moving electrons from the 5*d* to the 6*s* shell leads to a less negative value of the according maximum in $L(r)$. At the same time, considering a $5d^06s^2$ configuration adding one electron to the 6*s* orbital makes the weak shoulder in the negative Laplacian, which can be attributed to the sixth shell, disappear.

The ability to reconstruct the electronic configuration of an atom from the features shown by the Laplacian would be most important for the interpretation of electron densities obtained from experiment. For such an approach to be feasible, the differences in $L(r)$ for different configurations must be large enough to be unambiguously detectable in the experimental data. This means that when using reference data from quantum chemical calculations the effect due to a change in the valence configuration must exceed the typical deviations between theoretical and experimental topological electron density studies. This appears not to be the case for the La atom. Although the changes in $L(r)$ are large when expressed as percentages (about 30% relative to the single-CSF ground state calculation), the change in the absolute values is rather small (approximately 1 eÅ$^{-5}$). In recent experimental charge density studies[44,45,58] on compounds containing transition metals typical deviations between theory and experiment lie within a range of 0.77−1.13 eÅ$^{-5}$ which would make a clear detection of the differences discussed above difficult. It should be noted that the deviations between experimental and theoretical studies are to some extent due to inadequacies of the multipolar model which is commonly used for the reconstruction of the electron density from the measured structure factors. These shortcomings can be investigated by comparing the electron densities directly obtained from quantum chemical calculations with those obtained after applying a multipolar model to theoretical structure factors. Similar studies could show whether the precision which can be achieved within the multipolar model as it is used today is in principle accurate enough to reveal the differences in the Laplacian of the electron density due to diffferent electronic configurations.

## 5. Summary and Conclusion

In this study we have investigated the shell structure of isolated atoms as revealed by the Laplacian of the spherically averaged radial electron density. For heavy elements with $Z > 18$ the electronic shells are not observable as local maxima in the positive region of $L(r)$.[21−23,59] Our study has shown, however, that also local maxima with a negative sign of $L(r)$ are indicative for a shell. Special attention has been paid to the question whether different electronic configurations can be distinguished in $L(r)$. We could show that when considering also local maxima in the negative region of $L(r)$ as a signature of a electronic shell more than five shells can be observed. Furthermore, a detailed analysis then demonstrated that different electronic configurations may result in qualitative and quantitative changes in the Laplacian of the electron density. This would be of special importance for the interpretation of experimental studies. However, the results of our calculations suggest that the magnitude of the effects due to different electronic configurations is (currently) smaller than the deviations between the topological parameters obtained by quantum chemical calculations and by experiment.

**Acknowledgment.** The authors thank the Deutsche Forschungsgemeinschaft for the financial support within the SPP 1178 project Re1703/2-1. It is a pleasure for M.R. to acknowledge that it was made possible by the German science foundation DFG to continue funding in Switzerland after the relocation of M.R. from Jena to Zurich. We gratefully acknowledge inspiring discussions with Prof. Paul Ayers and thank Prof. Barbara Kirchner for an early reference to chapter 7.1.3 of Bader's book.

### References

(1) Ayers, P. W.; Morrison, R. C. *Acta Univ. Debreceniensis Ludovico Nominatae Ser. Phys. Chim.* **2002**, *34−35*, 197−216.

(2) Weinstein, H.; Politzer, P.; Srebrenik, S. *Theor. Chim. Acta* **1975**, *38*, 159−163.

(3) Angulo, J. C.; Dehesa, J. S. *Z. Phys. D − Atoms Clusters* **1993**, *25*, 287−293.

(4) Angulo, J. C.; Dehesa, J. S. *Phys. Rev. A* **1991**, *44*, 1516−1522.

(5) Angulo, J. C.; Yanez, R. J.; Romera, E. *Int. J. Quantum Chem.* **1996**, *58*, 11−21.

(6) Angulo, J. C.; Koga, T.; Romera, E.; Dehesa, J. S. *Theochem − J. Mol. Struct.* **2000**, *501−502*, 177−182.

(7) Esquivel, R. O.; Chen, J.; Stott, M. J.; Sagar, R. P.; Smith, V. H. *Phys. Rev. A.* **1993**, *47*, 936−943.

(8) Parr, R. G. *J. Chem. Sci.* **2005**, *117*, 613−615.

(9) Ayers, P. W.; Parr, R. G. *Int. J. Quantum Chem.* **2003**, *95*, 877−881.

(10) Lassettre, E. N. *J. Chem. Phys.* **1985**, *83*, 1709−1721.

(11) Hunter, G. *Int. J. Quantum Chem.* **1986**, *29*, 197−204.

(12) Kohout, M. *Int. J. Quantum Chem.* **2001**, *83*, 324−331.

(13) Wang, W.-P.; Parr, R. G. *Phys. Rev. A* **1977**, *16*, 891−902.

(14) Sperber, G. *Int. J. Quantum Chem.* **1971**, *5*, 189−214.

(15) Ayers, P. W.; Parr, R. G.; Nagy, A. *Int. J. Quantum Chem.* **2002**, *90*, 309−326.

(16) Cohen, L. *J. Chem. Phys.* **1979**, *70*, 788−789.

(17) Cohen, L. *J. Chem. Phys.* **1984**, *80*, 4277−4279.

(18) Cohen, L. *Phys. Lett. A* **1996**, *212*, 315−319.

(19) Hoffmann-Ostenhof, M.; Hoffmann-Ostenhof, T. *Phys. Rev. A* **1977**, *16*, 1782−1785.

(20) Bartell, L. S.; Brockway, L. O. *Phys. Rev.* **1953**, *90*, 833−838.

(21) Waber, J. T.; Cromer, D. T. *J. Chem. Phys.* **1965**, *42*, 4116−4123.

(22) Boyd, R. J. *J. Phys. B* **1976**, *9*, L69−L72.

(23) Sen, K. D.; Slamet, M.; Sahni, V. *Chem. Phys. Lett.* **1993**, *205*, 313−316.

(24) Becke, A. D.; Edgecombe, K. E. *J. Chem. Phys.* **1990**, *92*, 5397−5403.

(25) Kohout, M.; Wagner, F. R.; Grin, Y. *Int. J. Quantum Chem.* **2006**, *106*, 1499−1507.

(26) Bader, R. F. W.; MacDougall, P. J.; Lau, C. D. H. *J. Am. Chem. Soc.* **1984**, *106*, 1594−1605.

(27) Bader, R. F.; Essén, H. *J. Chem. Phys.* **1984**, *80*, 1943−1960.

(28) Sen, K. D.; Gayatri, T. V.; Krishnaveni, R.; Kakkar, M.; Toufar, H.; Janssens, G. O. A.; Baekelandt, B. G.; Schoonheydt, R. A.; Mortimer, W. J. *Int. J. Quantum Chem.* **1995**, *56*, 399−408.

(29) Coppens, P. *X-Ray Charge Densities and Chemical Bonding;* Oxford University Press: Oxford, New York, 1997.

(30) Gatti, C. *Z. Kristallogr.* **2005**, *220*, 399−457.

(31) Tsirelson, V. G.; Ozerov, R. P. *Electron Density and Bonding in Crystals;* Institute of Physics Publishing: Bristol, 1996.

(32) Koritsanszky, T. S.; Coppens, P. *Chem. Rev.* **2001**, *101*, 1583−1627.

(33) Coppens, P. A. V. *Acta Crystallogr.* **2004**, *A60*, 357−364.

(34) Sagar, R. P.; Ku, A. C. T.; Smith, V. H.; Simas, A. M. *J. Chem. Phys.* **1988**, *88*, 4367−4374.

(35) Shi, Z.; Boyd, R. J. *J. Chem. Phys.* **1988**, *88*, 4375−4377.

(36) Clementi, E.; Roetti, C. *At. Data Nucl. Data Tables* **1974**, *14*, 177−478.

(37) Kohout, M.; Savin, A.; Preuss, H. *J. Chem. Phys.* **1991**, *95*, 1928−1942.

(38) Hinze, J.; Jaffé, H. H. *J. Am. Chem. Soc* **1962**, *84*, 540−546.

(39) Hinze, J.; Jaffé, H. H. *Can. J. Chem.* **1963**, *41*, 1315−1328.

(40) Hinze, J.; Jaffé, H. H. *J. Phys. Chem.* **1963**, *67*, 1501−1506.

(41) Neese, F. *Inorg. Chim. Acta* **2002**, *337*, 181−192.

(42) Scherer, W.; Sirsch, P.; Shorokhov, D.; Tafipolsky, M.; McGrady, G. S.; Gullo, E. *Chem. Eur. J.* **2003**, *9*, 6057−6070.

(43) Scherer, W.; Eickerling, G.; Shorokhov, D.; Gullo, E.; McGrady, G. S.; Sirsch, P. *New J. Chem.* **2006**, *30*, 309−312.

(44) Scherer, W.; Eickerling, G.; Tafipolsky, M.; McGrady, G. S.; Sirsch, P.; Chatterton, N. P. *Chem. Commun.* **2006**, 2986−2988.

(45) Rohrmoser, B.; Eickerling, G.; Presnitz, M.; Scherer, W.; Eyert, V.; Hoffmann, R.-D.; Rodewald, U. C.; Vogt, C.; Pöttgen, R. *J. Am. Chem. Soc.* **2007**, *129*, 9356−9365.

(46) Reisinger, A.; Trapp, N.; Krossing, I.; Altmannshofer, S.; Herz, V.; Presnitz, M.; Scherer, W. *Angew. Chem., Int. Ed.* **2007**, *46*, 8295−8298.

(47) Hebben, N.; Himmel, H.-J.; Eickerling, G.; Herrmann, C.; Reiher, M.; Herz, V.; Presnitz, M.; Scherer, W. *Chem. Eur. J.* **2007**, *13*, 10078−10087.

(48) Reiher, M.; Hinze, J. Four-component ab initio Methods for Electronic Structure Calculations of Atoms, Molecules and Solids. In *Relativistic Effects in Heavy-Element Chemistry and Physics;* Hess, B. A., Ed.; Wiley-VCH: Weinheim, 2003; pp 61-88.

(49) Froese-Fischer, C. *The Hartree-Fock Method for Atoms: A Numerical Approach;* Wiley: Sussex, 1977.

(50) Grant, I. P. *Adv. Phys.* **1970**, *19*, 747−811.

(51) Helgaker, T.; Jorgensen, P.; Olsen, J. *Molecular Electronic-Structure Theory;* Wiley: Sussex, 2002.

(52) Margenau, H.; Murphy, G. M. *The Mathematics of Physics and Chemistry*, 2nd ed.; D. van Nostrand: Princeton, 1956; Vol. 1.

(53) Reiher, M. Ph.D. Thesis, University of Bielefeld, 1998.

(54) Andrae, D.; Reiher, M.; Hinze, J. *Int. J. Quantum Chem.* **2000**, *76*, 473−499.

(55) Andrae, D.; Hinze, J. *Int. J. Quantum Chem.* **1997**, *63*, 65−91.

(56) Bader, R. F. W. *J. Chem. Phys.* **1980**, *73*, 2871−2883.

(57) Moore, C. E. *Atomic Energy Levels Volume 2 and 3;* Nat. Stand. Ref. Data Ser.: Nat. Bur. Stand. 1971.

(58) Eickerling, G.; Mastalerz, R.; Herz, V.; Scherer, W.; Himmel, H.-J.; Reiher, M. *J. Chem. Theory Comput.* **2007**, *3*, 2182−2197.

(59) Bader, R. *Atoms in Molecules;* Clarendon Press: Oxford, 1990.

CT7002447